Vol 17 No 3, March 2008
1674-1056/2008/17(03)/1107-06
Chinese Physics B
© 2008 Chin. Phys. Soc.
and IOP Publishing Ltd

Investigation on the thermal radiation properties of antimony doped tin oxide particles

Fu Cheng-Wu(傅成武)[a)†], Zhang Shuan-Qin(张拴勤)[b)], and Chen Ming-Qing(陈明清)[a)]

[a)] *School of Chemical and Material Engineering, Southern Yangtze University, Wuxi* 214122, *China*

[b)] *The First Engineers Scientific Research Institute of the General Armaments Department, Wuxi* 214035, *China*

(Received 28 January 2007; revised manuscript received 19 October 2007)

This paper reports the preparation of antimony doped tin oxide crystalline powders by chemical coprecipitation method. The influence of sintering temperature and the sintering retention time on the thermal infrared emissivity is analysed. The thermal infrared reflectivity is measured and the optimum doping concentration is proposed.

Keywords: antimony-doped tin, sintered temperature, thermal radiation
PACC: 7280, 8140, 8100

1. Introduction

The thermal infrared (TIR) signatures of military field equipment are of increasing concern as technology which becomes available to detect these units at aircraft of satellite ranges. The threat of surveillance in TIR wavebands by line scan techniques has existed for many years, however advances in recent years have led to imaging techniques that give high quality images in real time. Such thermal images resulting from forward looking infrared systems may be used for both surveillance and target acquisition systems from either the ground or the air.

Two windows in the TIR region, 3 to 5μm and 8 to 14μm are of primary importance in missile and surveillance applications because these regions are relatively free of atmospheric absorption and energy can be transmitted over moderate distances. 3 to 5μm waveband is known as 'intermediate IR' and 8 to 14μm waveband as 'far IR'. The far IR enables much clearer imaging of objects which are close to the ambient background whereas the intermediate IR region is used when the object is much hotter than the surroundings such as hot exhaust pipes. Sensors operating in these two bands are the basis of some of the principal types of seekers in smart anti-armour munitions.[1]

Control of thermal emission in the TIR can be obtained for coatings which radiate in spectral regions not used for detection, however it has been suggested that this capability is costly and limited.[2] It is known from the Stefan–Boltzmann Law that the thermal emissivity ε of a coating contributes directly to its signature in the TIR region. To provide protection against sensing devices operating in the TIR spectral regions, camouflage materials with controlled thermal emissivities in the TIR regions to a level are necessary, where the camouflaged object has a similar thermal emissivity to its immediate surroundings. For example, vegetation typically has a thermal emissivity ε of about 0.5–0.6. Typically, materials which have a shiny or lustrous finish (such as metals) have a low thermal emissivity, a typical metallic lacquer having a thermal emissivity of about 0.5. Paints with metallic constituents are widely known, for example, in the automotive industry; however these do not provide good visual camouflage and also do not have a low thermal emissivity because the pigments used disrupt the action of the metallic particles. Conversely, materials with matt finishes provide good visual camouflage, but have a high thermal emissivity. Also most paint vehicles used today are brightly emitting in the TIR so that there is no real possibility of extending the spectral range just by adding pigment. It is felt[3] that the whole paint system, i.e. vehicle, pigments, fillers, etc, will have to be redesigned.

Organic pigments with their complex carbon–nitrogen–oxygen structures are strong TIR emitters. A number of the semiconductor fillers or pigments are relatively weak absorbers in the TIR region.[4] Their relatively weak thermal emissions in the TIR make

†E-mail: fuchwu-308 @163.com

them suitable for camouflage in this region. Tin antimony oxide is an antimony-doped semiconductor material, which has been mainly concerned with the use of optoelectronic devices such as solar cells, electroluminescence and liquid crystal displays of this material deposited on a glass or quartz substrate.[5−7] Burgard *et al* have given the results[8] of the effects of the Sb dopant concentration and heat treatment temperature from 400°C to 600°C with various sintering times. Putz *et al* have systematically studied the effects of the increasing rate of the sintering temperature on the microstructure and properties.[9] In this paper, antimony-doped tin oxide (ATO) is synthesized by the chemical co-precipitation method which is adaptable for fabricating ATO crystalline particles.[10] And the effect of sintering temperature on its infrared radiation properties is analysed, and the optimum sintering temperature and Sb doping content are indicated.

2. Experimental

2.1. Fabrication of ATO crystalline particles

SnO_2:Sb (ATO) particles were prepared by chemical co-precipitation. The $SnCl_4.5H_2O$ and $SbCl_3$ were each dissolved in hydrochloric acid. The acid solutions were then mixed in desired proportions and diluted with distilled water to 8 times the original volume. The solutions were slowly dripped into concentrated ammonium hydroxide. The PH was adjusted to between 8.5 and 9. Constant temperature bath was used to control the reactive temperature between 50°C and 60°C. The solution was agitated successively to the end of the reaction. Then the temperature was kept unchanged and cured for 2 hours, and pale yellow precipitate appeared. The precipitate was washed sequentially with water, filtered, dried under 80°C, and finally ground well. Pale yellow ATO particles are obtained. ATO particles are then sintered under different temperatures in the open air conditions. By changing the sintering temperature and the sintering preservation time, blue ATO particles with different infrared radiation properties are formed.

2.2. Measurement

2.2.1. TIR emissivity

ATO particles and binders are blended in the mill boxer by the weight ratio of 1 to 1. After ATO particles in binders are thoroughly ground and dispersed, the pressure-fed spray gun is used to spray the paint onto a copperplate paper. The thickness of the coating is thick enough to ensure the measured emissivity being that of ATO coating. After the coating is sufficiently dried, its TIR emissivity in the 8–14μm is measured. IRE-1 Infrared Emission Thermometer is used to measure the TIR emissivity of coatings under the temperature 50°C. In order to make the emissivity of the binder have less influence on that of the coating, here the binder should meet the high infrared transparency and is specifically synthesized.[11] The TIR transparency of binder is measured by the GXIII FLIRS. Figure 1 shows the infrared transparency of the binder. It is shown that the infrared transparency of the binder is about 80% in the wavelength range 8–14μm (corresponding to the wavenumber range of $\sim$700$\sim$1250cm^{-1}). If there is no special explanation, in this paper the TIR emissivity all refers to that of the coating composed of the infrared binder and ATO particles.

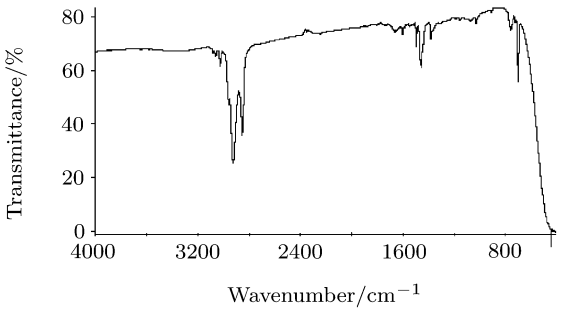


Fig.1. The infrared transparency of the binder.

2.2.2. The microstructure analysis

The morphology of ATO crystalline particles was observed on high resolution transmission electron microscope (JEM-1200EX II type made by Japan).

The crystalline phases, microstructures and compositions are identified by x-ray diffractometer (XRD) (Rigaku K/max 2550 VB/PC made in Japan).

Particle size of the ATO crystalline particles is analysed with Laser Diffraction Analyser (made by Beckman Coulter Company in America).

2.2.3. Thermal infrared reflectivity

ATO particles are pulverized into pallets with the thickness of 1mm at the pressure of 20MPa. The in-

frared reflectivity ρ is measured by FTIR (IFS 113V FTIR made by Bruker Company).

3. Results and discussion

3.1. The influence of the sintering temperature

As reported in Refs.[11–13], the electrical resistance, optical properties, and microstructure and macroscopic properties of ATO coatings are mainly influenced by the sintering temperature with various heating time and antimony doping level. In this paper we also mainly concentrate on the influence of the sintering temperature and Sb doping concentration on the infrared emissive properties of ATO particles.

Figure 2 shows the particle size and shape of ATO particles under different sintering temperatures for 80°C (drying), 1000°C, 1200°C and 1300°C respectively. It is shown that the particle size of ATO particles dried under 80°C is relatively smaller. When the sintering temperature is 1000°C, the average particle size is about 30–40nm, and the particle is of the irregular ellipsoid shape. When the sintering temperature is increased to 1200°C, the particle size is increased rapidly to 100nm. Also edges and corners appear at the periphery of the particle, which indicates that the crystalline structures tend to be perfect and the grain

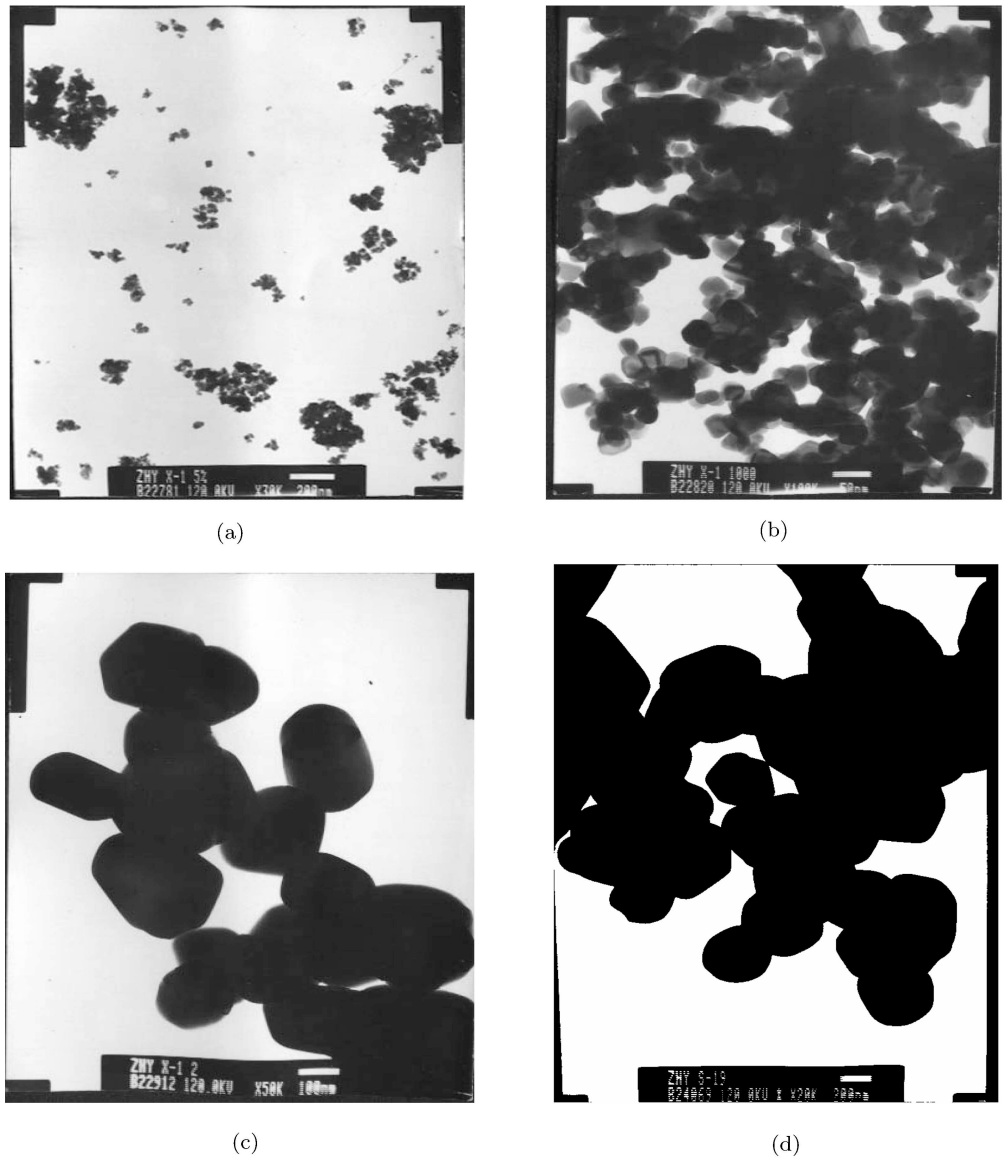


Fig.2. The micrograph of ATO crystalline particles.

shape changes no more. When the sintering temperature reaches 1300°C, the average particle size is of 300nm. Further increasing the sintering temperature, we find that the particle size of ATO is nearly unchanged, because the crystalline structure of ATO particle has been perfect and every grain is an independent ellipsoid.

Figure 3 shows the influence of the sintering temperature on the infrared emissivity ε. When the sintering temperature is lower than 1000°C, ε is higher than 0.90. With increasing the sintering temperature continuously to 1200°C, ε begins to decrease. When the sintering temperature is increased to 1350°C, ε is reduced to its lowest value 0.68. With increasing the sintering temperature further, ε begins to rise. Therefore the optimum sintering temperature is between 1300–1350°C for fabricating ATO crystalline particles with low infrared emissivity. For further investigations, the particles with the lowest infrared emissivity are used.

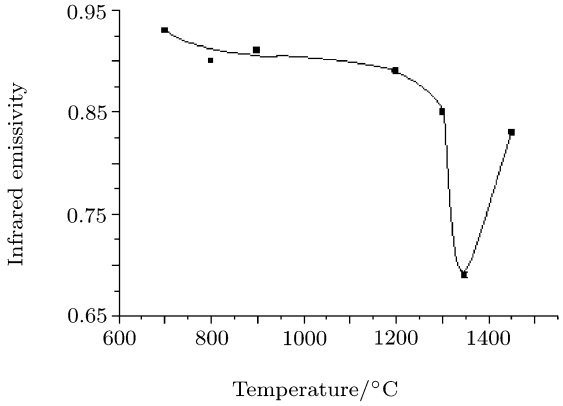


Fig.3. The effect of the sintering temperature on the infrared emissivity.

Figure 4 shows the XRD spectroscopy of ATO crystalline particles under the sintering temperature of 1300°C. It is shown that the XRD pattern of ATO sample sintered under 1300°C is similar with that of the tetragonal structured SnO_2. Three strong diffraction peaks corresponding to the crystalline faces (110), (101), and (211) also correspond to that of the tetragonal structured SnO_2. The cell parameters are a=0.33581nm, b=0.26498nm and c=0.17673nm respectively, which means that no new phase is introduced with Sb doping , and only a little peak shift appears for ATO particles. It is concluded that Sb ions merged into SnO_2 crystalline structure completely.

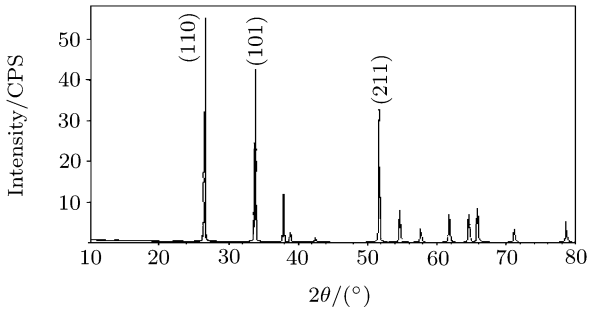


Fig.4. XRD patterns of as-prepared ATO product.

Figure 5 shows the effect of the sintering retention time on the particle diameter distribution of ATO sample 1 and 2. Both samples are sintered at 1300°C, but sample 1 with a holding time of 2h and sample 2 of 4h. Table 1 shows the particle size computed and the TIR emissivity measured.

Table 1. Particle size distribution and the infrared emissivity.

sample	sintering temperature/°C	sintering holding time/h	average particle size/nm	median diameter/nm	TIR ε
1	1350	2	100	75	0.82
2	1350	4	300	240	0.68

It is shown that the average particles size of sample 1 is 100nm, the medium diameter is 75nm; the average particles size of sample 2 is 300nm, the medium diameter is 240nm. The emissivity for sample 1 and 2 are 0.82 and 0.68 respectively. Therefore it can be considered that with increasing the sintering preservation time, the average size of ATO particles is increased, and the crystalline structure is more perfect. Larger particle size and a more perfect crystalline structure are favourable for the reduction of the TIR emissivity of the sample, which is consistent with the results reported by Xu *et al* that large particle size increases the scattering and reduces the absorption of the incident infrared radiation and so leads to the reduction of the TIR emissivity.[14]

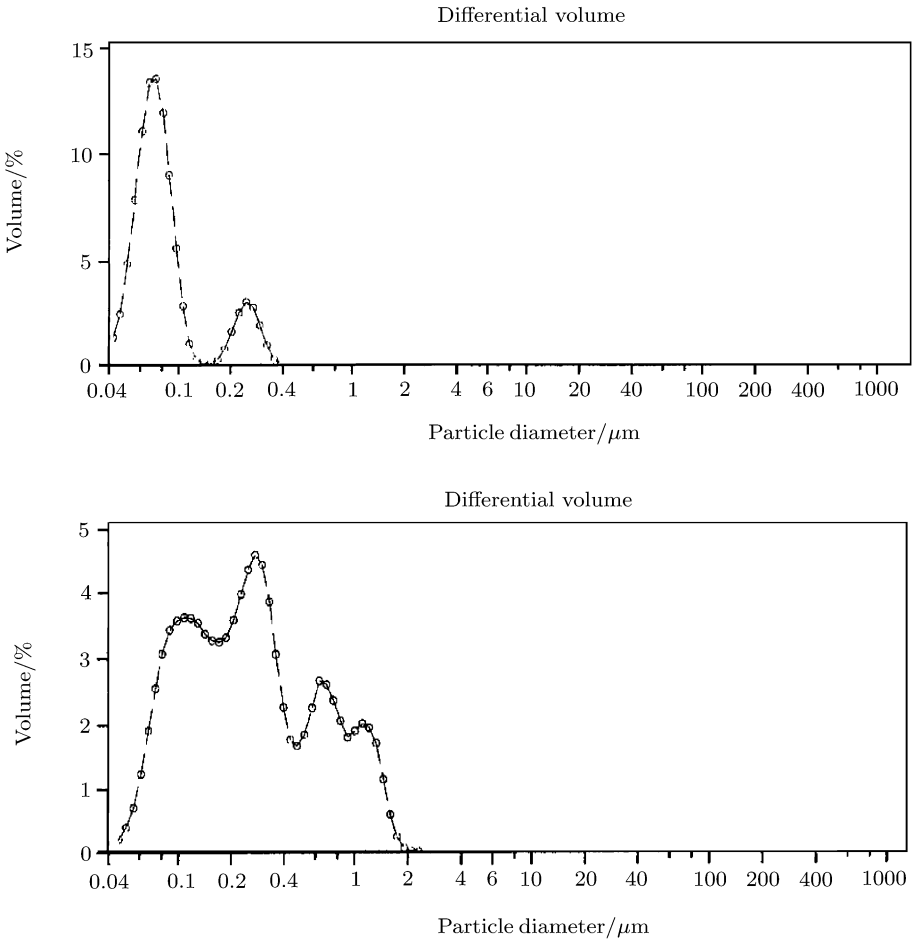


Fig.5. Effect of the sintering preservation time on the particle diameter distribution.

3.2. Effect of Sb-doping concentration on the TIR reflectivity

It is known that the charge carrier density has an important influence on the TIR reflectivity ρ ($\rho = 1 - \varepsilon$). The infrared reflectivity for ATO pallets with different Sb doping concentration is measured and shown in Fig.6. It is shown that ATO pallets with 2% and 4% Sb doping concentration have the higher reflectivity of 0.325. The reflectivity is reduced by increasing or decreasing Sb doping concentration further, e.g. 10% Sb doping or 1% Sb doping. Therefore, it can be deduced that the optimum Sb doping concentration is in the range of 2% to 4%, which is favourable for ATO materials with low TIR emissivity.

The reflecting properties in the IR region for ATO can be explained by Drude's theory which describes the relation of the carrier concentration determining the plasma wavelength (λ_p). For $\lambda > \lambda_p$, it leads to high reflectivity.

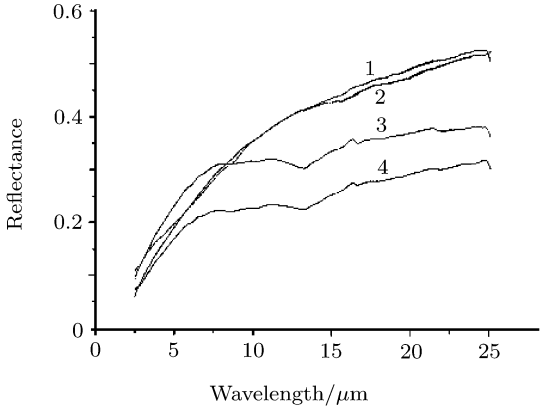


Fig.6. The relationship between the TIR reflectivity and Sb doping concentration. Sb doping concentration: curve 1: 2%, curve 2: 4%, curve 3: 10% and curve 4: 1%.

Also carrier concentration governs the maximum achievable reflectivity in the infrared region. The higher carrier concentration, the higher is the maximum achievable reflectivity. As previously mentioned and evidenced,[15,16] when the Sb doping content is lower, Sb^{5+} dominates to lead to increase of the carrier concentration. So in our figure, the reflectivity for Sb 2% content is higher than that of Sb 1% content. But with Sb doping concentration increasing further to 4% or higher, the carrier concentration varies less.[12,13] Conversely the Sb^{3+} component appears and its percentage is more and more important existing as impurity, which induces increase of the TIR emissivity,[17] or, in other words, decrease of the TIR reflectivity.

4. Conclusions

(1) ATO crystalline powders are synthesized by chemical coprecipitation method. By controlling the sintering temperature and the sintering maintenance time, ATO powders with different TIR emissivity and particle size distribution are obtained.

(2) The sintering temperature has an observable influence on the TIR emissivity. The optimum sintering temperature is about 1350°C, under which the TIR emissivity of ATO synthesized is 0.68.

(3) The sintering maintenance time has a main influence on the particle size distribution of ATO crystalline powders. Under 1350°C sintering temperature the longer sintering maintenance time is helpful for the growth of ATO particle size and more perfect crystalline structure, which is useful for reducing the TIR emissivity of ATO coating.

(4) Sb doping is the source of charge carrier which determines mainly the TIR reflectivity. 2%∼4% Sb doping concentration is proposed to be an optimum.

References

[1] Ogorkiweicz R W 1989 *Int. Defense Rev.* **22** 53

[2] Brunswick C 1995 *Guide to Camouflage for DARCOM Equipment Developers* Report Prepared for MERADCOM under Contract DAAG 53-76-C-0126

[3] Raisbeck G, Aronson J R and Key M E 1997 *Design Goals for Future Camouflage Systems* AD-A099-223

[4] Lofgren Per-Ake 1987 *Camouflage Concepts for the Nineties, Proc. International Conference on Polymers in Defence* **17** 1

[5] Wagner S and Carlson D E 1991 *Proc. 10th European Photovoltaic Solar Energy Conference* (Lisbon) p1179

[6] Arai Y, Ishii M, Shinohara H and Yamazaki S 1991 *IEEE Electro. Dev. Lett.* **12** 460

[7] Kumar S and Drevillon B 1989 *J. Appl. Phys.* **65** 3023

[8] Burgard D, Goebbert C and Nass R 1998 *J. Sol-Gel Sci. Technol.* **13** 789

[9] Putz J, Ganz D and Gasparro G C 1998 *J. Sol-Gel Sci. Technol.* **13** 1005

[10] Vincent C A and Weston D G C 1972 *J. Electrochem. Soc.: Solid State Sci. Technol.* **119** 518

[11] Colin A V and Derek G C 1972 *J. Electrochem. Soc.: Solid State Sci. Technol.* **119** 518

[12] Terrier C, Chatelon J P and Roger J A 1997 *Thin Solid Films* **295** 95

[13] Zu X T 2006 *Chin. Phys.* **15** 75

[14] Xu W L and Shen S C 1992 *Appl. Opt.* **31** 4488

[15] Srinivasa M N and Jawalekar S R 1983 *Thin Solid Films* **108** 277

[16] Shanthi E, Banerjee A, Dutta V and Chopra K L 1982 *J. Appl. Phys.* **53** 1615

[17] Howson R P and Ridge M I 1981 *Thin Solid Films* **77** 119